

1 **A genomic resource for exploring bacterial-viral dynamics in seagrass ecosystems**

2
3 Cassandra L. Ettinger^{1, #}, Jason E. Stajich^{1, 2}

4
5 ¹Department of Microbiology and Plant Pathology, University of California, Riverside, CA, United
6 States

7
8 ²Institute for Integrative Genome Biology, University of California, Riverside, CA,
9 United States

10
11 **#Corresponding Author:** Cassandra L. Ettinger, cassande@ucr.edu

12
13 **Keywords:** *Zostera marina*, eelgrass, metagenomics, viral discovery, viral diversity, phage,
14 bacteria, carbon cycling, metagenome-assembled genomes

15

16

17

18

19

20

21

22

23

24

25

26

27

28

29

30

31

32

33

34

35

36

37

38

39

40

41

42

43 **Abstract:**
44
45 **Background:** Seagrasses are globally distributed marine flowering plants that play foundational
46 roles in coastal environments as ecosystem engineers. While research efforts have explored
47 various aspects of seagrass-associated microbial communities, including describing the
48 diversity of bacteria, fungi and microbial eukaryotes, little is known about viral diversity in these
49 communities.

50
51 **Results:** To begin to address this, we leveraged metagenomic sequencing data to generate a
52 catalog of bacterial metagenome-assembled genomes (MAGs) and phage genomes from the
53 leaves of the seagrass, *Zostera marina*. We expanded the robustness of this viral catalog by
54 incorporating publicly available metagenomic data from seagrass ecosystems. The final MAG
55 set represents 85 high-quality draft and 62 medium-quality draft bacterial genomes. While the
56 viral catalog represents 354 medium-quality, high-quality, and complete viral genomes.
57 Predicted auxiliary metabolic genes in the final viral catalog had putative annotations largely
58 related to carbon utilization, suggesting a possible role for phage in carbon cycling in seagrass
59 ecosystems.

60
61 **Conclusions:** These genomic resources provide initial insight into bacterial-viral interactions in
62 seagrass meadows and are a foundation on which to further explore these critical interkingdom
63 interactions. These catalogs highlight a possible role for viruses in carbon cycling in seagrass
64 beds which may have important implications for blue carbon management and climate change
65 mitigation.

66
67
68
69
70
71

72 **Background:**

73
74 Seagrasses are submerged marine flowering plants that have critical roles as foundation
75 species in coastal ecosystems worldwide. They provide essential ecosystem services such as
76 stabilizing the seafloor, filtering pollutants, supporting fisheries, and driving biogeochemical
77 cycles [1–3]. One of their most significant contributions is their ability to sequester carbon in
78 both their tissues and surrounding sediments (i.e., blue carbon) [2,4]. Despite their ecological
79 importance, seagrass ecosystems are under increasing threat from pollution, climate change,
80 and coastal development. Preserving these ecosystems is critical not only for their carbon
81 sequestration potential but also for maintaining the biodiversity and ecological services they
82 provide to coastal communities.

83

84 In recent years, there has been growing recognition of the importance of microorganisms in
85 maintaining the health of plants [5–7]. Studies have begun to describe the composition and
86 structure of the bacterial community associated with seagrasses, particularly *Zostera marina*,
87 the dominant seagrass in the Northern hemisphere [8–14]. These bacterial communities are
88 thought to have important roles in facilitating nitrogen and sulfur cycling to benefit seagrass
89 growth and survival [8,9,11,12,15–17].

90

91 While research has largely focused on the bacterial component of these microbial communities,
92 advances in sequencing and bioinformatics now allow us to explore the role of viruses in these
93 systems. Phages, in particular, have been shown to influence global ocean and soil
94 biogeochemical cycles by modulating host population dynamics through auxiliary metabolic
95 genes (AMGs), which can directly alter bacterial metabolism to increase overall host fitness [18–
96 21]. However, the diversity and ecological roles of phage in seagrass ecosystems remains
97 largely unexplored.

98

99 In this study, we generated a catalog of viruses from seagrass-associated metagenomic
100 samples, and then investigated host-viral dynamics of viral operational taxonomic units (vOTUs)
101 and bacterial metagenome-assembled genomes (MAGs) generated from *Z. marina* leaf
102 samples from Bodega Bay, CA. Specifically our objectives were to: (i) create a catalog of
103 vOTUs from *Z. marina* and other seagrass species using publicly available metagenomic
104 sequencing data, (ii) assemble a catalog of bacterial MAGs from *Z. marina* leaf tissue, and (iii)
105 explore bacterial-phage dynamics with a focus on exploring AMGs involved in nitrogen and
106 sulfur metabolisms.

107

108 **Methods:**

109

110 *Sequence generation*

111

112 We extracted DNA from epiphytic washes from *Z. marina* leaves as part of previous work
113 focused on characterizing the mycobiome using high-throughput sequencing of the ITS2 region
114 [22]. We chose three DNA extracts from that work here for deep metagenomic sequencing with
115 the goal of obtaining high quality metagenome-assembled genomes. We provided DNA to the
116 UC Davis Genome Center DNA Technologies Core for sequencing and library preparation. DNA
117 libraries were sequenced on an Illumina HiSeq4000 to generate 150 bp paired-end reads.

118

119 *Metagenomic processing*

120

121 We trimmed sequence reads using bbduk v. 37.68 [23] with the following parameters: qtrim=rl
122 trimq=10 maq=10. We then mapped against and removed any reads from the metagenomes
123 matching the available genome for *Z. marina* v. 3.1 [24] using bowtie2 v. 2.4.5 [25] and
124 samtools v. 1.11 [26]. We co-assembled the remaining reads from all three metagenomic
125 samples using MEGAHIT v. 1.2.9 [27].

126

127 We identified and assessed metagenome-assembled genomes (MAGs) using the anvi'o v. 7.2
128 workflow [28]. First, we used bowtie2 v. 2.4.5 [25] and samtools v. 1.11 [26] to obtain read
129 coverage for each metagenomic sample against the assembly. Then we used “anvi-gen-
130 contigs-database” to generate a database from the co-assembly and to predict open-reading
131 frames using Prodigal v. 2.6.3 [29]. This command also identifies single-copy bacterial [30],
132 archaeal [31], and protista [32] genes using HMMER v. 3.2.1 [33] and ribosomal RNA genes
133 using barrnap [34]. We predicted taxonomic assignments for each gene call using Kaiju v. 1.8.2
134 [35] with the NCBI BLAST non redundant protein database nr including fungi and microbial
135 eukaryotes v. v. 2020-05-25. For each individual metagenomic sample, we then used “anvi-
136 profile” to construct an anvi'o profile for contigs >1 kbp with the “–cluster-contigs” option. Next
137 we ran several automatic binning algorithms including MetaBAT2 v. 2.15, MaxBin v. 2.2.1,
138 BinSanity v.0.5.4 and CONCOCT v. 1.1.0 [36–39] to generate preliminary sets of bacterial
139 MAGs. We provided the resulting set from each algorithm to DAStool v. 1.1.2 [40] to generate a
140 single optimal MAG set. MAGs from this set were then manually assessed for contamination
141 and refined using “anvi-refine”. After manual refinement, MAGs were further de-contaminated
142 using MAGpurify v. 2.1.2 [41].

143

144 We assessed MAG completeness and contamination using CheckM v. 1.2.1 [42] and CheckM2
145 v. 1.0.1 [43]. In this work we report all identified MAGs with >80% completion and <10%
146 contamination. We refer to MAGs as high quality if they were >90% complete with <5%
147 contamination, and medium quality if they were >50% complete with <10% contamination per
148 established guidelines [44]. To obtain a putative taxonomy for each MAG, we used GTDB-Tk v.
149 2.2.6 [45], which uses a combination of average nucleotide identity and phylogenetic placement
150 in the context of the Genome Taxonomy Database to taxonomically identify MAGs.

151

152 *Viral identification*

153
154 In order to have a robust dataset to compare our recovered virus catalog in the context of other
155 studies, we downloaded publicly available data from NCBI GenBank from nine studies
156 [11,12,17,46–51] representing 65 metagenomic and 18 metatranscriptomic samples collected
157 from seagrass environments (Table S1).

158
159 We filter and trimmed public metagenomic data using bbDuk v. 37.68 [23] with the following
160 parameters: ktrim=r k=23 mink=11 hdist=1 tpe tbo qtrim=rl trimq=10 maq=10. Then for each
161 study, samples were co-assembled using MEGAHIT v. 1.2.9. We used the co-assemblies for
162 each study, as well as the co-assembly from this study, when identifying viral sequences using
163 a workflow similar to Guo et al. [52]

164
165 Briefly, we identified viral sequences from metagenomic co-assemblies using VirSorter2 v. 2.2.3
166 [53], a tool that uses multiple random forest classifiers to predict whether a sequence contains a
167 DNA or RNA virus, with the following parameters: --min-length 5000, --min-score 0.5, --include-
168 groups dsDNAPhage, RNA, ssDNA, lavidaviridae. We then ran CheckV v0.8.1 [54] on the
169 VirSorter2 predicted viral sequences using the “end_to_end” workflow. To be conservative in
170 our analyses, we removed viral sequences with a CheckV quality score of “not-determined” and
171 “low-quality” prior to downstream analysis. We then ran VirSorter2 again on the viral sequences
172 from the CheckV workflow with the --prep-for-dramv option. We used DRAM-v v. 1.2.2 [55] to
173 “annotate” viral sequences and then “distill” annotations into predicted auxiliary metabolic genes
174 (AMGs) for phage.

175
176 *Virus clustering and analysis*
177

178 We clustered viral sequences \geq 10 kbp in length into 95% similarity viral operational taxonomic
179 units (vOTUs) using dRep v. 3.2.2 [56]. We used Prodigal v. 2.6.3 [29] to predict open reading

180 frames in vOTUs using the -p meta option. We then provided the predicted proteins from the
181 phage vOTUs to VContact2 v. 0.9.19, as well as predicted proteins from the INPHARED August
182 2023 viral reference database, to generate viral clusters (VCs) based on viral gene-sharing
183 networks [57,58]. We further used geNomad v. 1.7.4 to assign taxonomy to phage vOTUs [59].
184 We used iPhoP v. 1.3.2 [60], which integrates across multiple methods in a machine learning
185 framework to assign host taxonomy at the genus level, to predict host-virus linkages using a
186 combination of the final bacterial MAG collection from this study and iPhoP's reference host
187 database.

188

189 We mapped reads from each metagenome to vOTUs using bowtie2 --sensitive with a
190 minid=0.90 to quantify vOTU relative abundance [61]. We then used SAMtools and BEDTools
191 genomecov to obtain coverage estimates for each vOTU across each individual metagenomic
192 sample [26,62]. We used coverM in contig mode to parse bam files and calculate the trimmed
193 pileup coverage (tpmean) of vOTUs which displayed $\geq 75\%$ coverage over the length of the viral
194 sequence. Thresholds for analysis of vOTUs were based on community guidelines for length
195 (i.e. ≥ 10 kbp), similarity (i.e. $\geq 95\%$ similarity), and detection (i.e. $\geq 75\%$ of the viral genome
196 length covered $\geq 1x$ by reads at $\geq 90\%$ average nucleotide identity) [63,64]. The viral relative
197 abundance (tpmean), CheckV quality, geNomad taxonomy, iPhoP host-prediction, MAG
198 diversity, and DRAM-v annotation results were analyzed and visualized in R v. 4.3.0 [65] using
199 the tidyverse v. 2.0.0 and phyloseq v. 1.44.0 [66,67].

200

201 To compare viral diversity between metagenomic samples (i.e. beta diversity), we calculated the
202 Hellinger distance, the Euclidean distance of Hellinger transformed relative abundance (tpmean)
203 data. We performed Hellinger transformations using the transform function in the microbiome v.
204 1.22.0 package [68], calculated the Hellinger distance using the ordinate function in phyloseq,
205 and then visualized these distances using principal-coordinate analysis (PCoA).

206

207 **Results and Discussion**

208

209 *Refined viral catalog from seagrass ecosystems*

210

211 In total, we recovered 17,145 predicted viral genomic fragments which we clustered at 95%
212 average nucleotide identity into 3,633 vOTUs. To ensure a high quality viral catalog, we filtered
213 this dataset further using community thresholds for length and quality [63,64]. The refined viral
214 collection represents 354 viral sequences comprising 351 double-stranded DNA phage, two
215 lavidaviridae, and one RNA phage based on VirSorter2 random forest classification, with each
216 sequence representing a unique vOTU (Table S2). Of these sequences, nine are integrated
217 prophage (Figure 1A). The final catalog includes 44 complete, 28 high-quality and 282 medium-
218 quality draft viral genomic fragments (Figure 1B).

219

220 To explore the taxonomy of the viral sequences reported here, we used two complementary
221 approaches: VContact2 [57], a cluster based method, and geNomad [59], an alignment based
222 tool. We ran VContact2 [57] with INPHARED [58] reference genomes to cluster phage vOTUs
223 into 136 VCs, which represent genus-level groupings based on gene-sharing networks. Of
224 these, 35 VCs represented clusters that contained reference genomes, while the other 101 VCs
225 were unique, potentially representing novel phage genera (Figure S1A). However, 148 vOTUs
226 could not be assigned confidently to any VC.

227

228 Taxonomic classification of viruses was further refined using geNomad [59]. Most vOTUs
229 (98.58% of vOTUs) were assigned to the *Caudoviricetes* class of tailed double-stranded DNA
230 bacteriophage (Figure S1B). However, viral taxonomy is currently in revision [69], and the
231 majority of sequences could not be confidently placed into finer taxonomic ranks: 331 vOTUs
232 were unclassified at the order level, and 352 at the family level. While geNomad provided

233 higher-level taxonomic predictions for 351 of the 354 vOTUs, more comprehensive classification
234 awaits future updates to formal viral taxonomy definitions.

235

236 The recovery of phage genomes from metagenomes varied across experimental studies (Figure
237 1C). Of the 354 viral sequences in the final catalog, 50 were recovered from the new
238 metagenomic data in this study, with the remainder derived from publicly available
239 metagenomes. Studies that contributed more viral sequences to the final catalog generally
240 employed deeper sequencing, with average depths ranging from 9.7 to 28.2 Gb per sample,
241 compared to studies with few recovered viral sequences (1.2 to 9.5 Gb per sample).

242

243 When we examined viral community composition across metagenomes, clustering by scientific
244 study was evident (Figure 1D). Notably, the viral communities in the metagenomes generated in
245 this study formed a distinct cluster. However, technical differences (e.g., sequencing depth)
246 across datasets prevented us from drawing broader conclusions regarding viral diversity based
247 on seagrass species or tissue type.

248

249 Despite the use of deep metagenomic sequencing and the integration of public metagenomes,
250 we recovered a relatively small, refined catalog of viral sequences. This highlights the limitations
251 of relying solely on short-read metagenomic sequencing to capture viral diversity, at least in
252 seagrass ecosystems. Viromics approaches (e.g., [70]) may provide more comprehensive
253 insights into these viral communities, as even with improved bioinformatics pipelines, true viral
254 diversity and abundance remains elusive.

255

256 *MAG collection reflects abundant bacterial groups on Z. marina leaves*

257

258 We assembled 147 total bacterial MAGs including 85 high-quality draft MAGs (>90%
259 completion, <5% contamination), and 62 medium-quality MAGs (>80% completion, <10%

260 contamination) (Table S3). These MAGs largely belong to the following taxonomic classes
261 (Figure 2A): Alphaproteobacteria (43), Gammaproteobacteria (35), Bacteroidia (29), and
262 Planctomycetia (16). Within these classes, the most frequently recovered orders were:
263 Rhodobacterales (28), Pirellulales (14), Flavobacterales (12), Chitinophagales (11) and
264 Pseudomonadales (11). Notably, using GTDB-Tk 30 MAGs could not be assigned to any known
265 genus, six were unclassified at the family level, and one lacked an assignment at the order
266 level, highlighting potential evolutionary novelty compared to the current GTDB database. These
267 findings suggest that seagrass ecosystems may harbor novel bacterial species that remain
268 uncharacterized.

269

270 The taxonomic distribution of the recovered MAGs is broadly consistent with previous DNA-
271 based surveys of *Zostera*-associated bacteria. These studies also identified
272 Alphaproteobacteria, Gammaproteobacteria, and Bacteroidia as dominant classes, along with
273 orders such as Rhodobacterales and Flavobacterales [9–13]. Further a global study of *Z.*
274 *marina* reported that Planctomycetia was enriched on leaves relative to surrounding water [8].
275 Together, these results suggest that this MAG collection complements previous DNA-based
276 surveys, providing an opportunity for exploring deeper insight into the genomics and functional
277 potential of abundant bacterial taxa within *Z. marina* ecosystems.

278

279 *Recovered phage largely predicted to infect most frequent MAG phyla*

280

281 We used iPhoP [60] to predict bacteria-virus linkages but were only able to predict bacterial
282 hosts for 18 vOTUs (Figure 2B). Of these, hosts generally were distributed across the most
283 frequently recovered MAG classes (i.e., Alphaproteobacteria, Gammaproteobacteria, and
284 Bacteroidia). While the MAG collection was added to the iPhoP database to enable prediction
285 of direct links between MAGs and viruses, only one MAG, SGMAG-05 (a Saprospiraceae
286 bacterium in the class Bacteroidia) was predicted to be host to a virus from the high-quality

287 catalog. This phage, vOTU566, was identified as a prophage belonging to the Caudoviricetes.
288 The remaining host-virus predictions were derived from iPHoP's default genome library rather
289 than the MAG collection. The limited number of host-virus links identified between the MAG and
290 viral collections suggests that much more work remains to uncover these interactions within
291 seagrass ecosystems. Future studies should endeavor to sequence the bacterial community
292 alongside deeper virome sequencing to better capture viral diversity. Additionally, employing
293 physical linking techniques such as Hi-C may help characterize novel host-viral interactions.

294
295 *Auxiliary metabolic genes point to phage role in carbon cycling*
296

297 We used DRAM-v [55] to explore predicted AMG functions in the viral collection (Figure 2C).
298 Over half of putative AMGs were unannotated (57.47%), similar to other recent studies of phage
299 from the environment [71,72]. Given the importance of nitrogen and sulfur cycling in seagrass
300 ecosystems, we searched the annotated AMGs for putative functions related to these
301 processes. However no annotated AMGs had predictions related to nitrogen fixation or sulfur
302 cycling. This absence could be biological (e.g., such genes may be more likely to be present in
303 root or rhizosphere samples vs. leaves) or could reflect the limitations of recovering viruses from
304 metagenomic datasets. Virome sequencing will likely be necessary to confirm whether viruses
305 play a role in these nutrient cycles.

306
307 In contrast, we identified a variety of predicted AMGs with putative annotations of functions
308 related to carbon utilization, particularly carbohydrate-active enzymes (CAZymes) involved in
309 organic carbon cycling, sugar processing and plant degradation (Figure 2D). Seagrass beds are
310 known as hot spots for carbon sequestration and key contributors to blue carbon storage [2,4].
311 Additionally previous work in the Mediterranean seagrass *Posidonia oceanica* has shown that
312 rhizosphere sediments are enriched in sugars [46]. These findings may suggest a possible role

313 for viruses in carbon cycling in seagrass beds, which may have important implications for blue
314 carbon management and climate change mitigation.

315

316 **Conclusion**

317

318 This study provides a valuable community resource and catalog of refined seagrass-associated
319 bacterial and viral genomes, serving as a genomic foundation for future research. These
320 comprehensive collections likely capture the most abundant groups associated with the leaves
321 of *Z. marina*. While we found no evidence of AMGs related to nitrogen or sulfur metabolism, we
322 instead report the presence of AMGs putatively linked to carbon utilization, particularly a diverse
323 array of CAZymes that may be involved in organic carbon cycling. These results suggest that
324 viruses may play an important role in carbon sequestration and blue carbon storage within
325 seagrass ecosystems, which may have significant implications for climate change mitigation.

326 Moving forward, research should prioritize investigating the role of phages through viromic
327 techniques, which would offer deeper insights into viral ecology and phage contributions to
328 carbon cycling in seagrass habitats.

329

330

331

332

333

334

335

336

337

338

339 **Declarations**

340 *Ethics approval and consent to participate*

341 Not applicable.

342 *Consent for publication*

343 Not applicable.

344 *Availability of data and material*

345

346 The raw metagenomic sequencing data was deposited at GenBank under accession no.

347 [PRJNA1140276](#). MAGs with > 90% completion estimates were deposited on NCBI under this

348 BioProject at GenBank under accession no. [PRJNA1140276](#), while MAGs with completion

349 estimates between 80 and 90% were deposited on Zenodo (DOI: [10.5281/zenodo.14225973](#)).

350 Viral genomes were also deposited on Zenodo (DOI: [10.5281/zenodo.14226038](#)). All code used

351 in this work has been deposited on Github ([casett/Seagrass_MAG_and_Virus_Catalog](#)) and

352 archived in Zenodo (DOI: [10.5281/zenodo.14226514](#)).

353

354 *Competing Interests*

355

356 The authors declare no competing interests.

357

358 *Funding*

359

360 The sequencing data in this work was generated by grants from the UC Davis H. A. Lewin

361 Family Fellowship and the UC Davis Center for Population Biology to CLE. CLE was supported

362 by the National Science Foundation (NSF) under a NSF Ocean Sciences Postdoctoral

363 Fellowship (Award No. 2205744). JES is a CIFAR Fellow in the program Fungal Kingdom:

364 Threats and Opportunities and was partially supported by NSF awards EF-2125066 and IOS-

365 2134912. Computations were performed using the computer clusters and data storage

366 resources of the UC Riverside HPCC, which were funded by grants from NSF (MRI-2215705,
367 MRI-1429826) and NIH (1S10OD016290-01A1). The funders had no role in study design, data
368 collection and analysis, decision to publish, or preparation of the manuscript.

369 *Authors' Contributions*

370
371 CLE conceived and designed the experiments, performed sampling, analyzed the data,
372 prepared figures and/or tables, wrote and reviewed drafts of the paper. JES reviewed drafts of
373 the paper.

374 *Acknowledgements*

375
376 We would like to thank Jonathan A. Eisen for feedback on this manuscript. We would like to
377 thank Katherine Dynarski ([ORCID: 0000-0001-5101-9666](https://orcid.org/0000-0001-5101-9666)) and Sonia Ghose ([ORCID: 0000-0001-5667-6876](https://orcid.org/0000-0001-5667-6876)) for their help with sample collection. We would also like to thank John J.
378 Stachowicz for use of his scientific sampling permit, California Department of Fish and Wildlife
379
380 Scientific Collecting Permit # SC 4874.

381
382
383
384
385
386
387
388
389
390
391
392
393
394
395
396
397

398 **References**

399 1. Hemminga MA, Duarte CM. *Seagrass Ecology*. Cambridge University Press; 2000.
400 doi:10.1017/CBO9780511525551

401 2. Fourqurean JW, Duarte CM, Kennedy H, Marbà N, Holmer M, Mateo MA, et al. Seagrass
402 ecosystems as a globally significant carbon stock. *Nat Geosci*. 2012;5: 505–509.
403 doi:10.1038/ngeo1477

404 3. Orth RJ, Carruthers TJB, Dennison WC, Duarte CM, Fourqurean JW, Heck KL, et al. A
405 Global Crisis for Seagrass Ecosystems. *BioScience*. 2006;56: 987. doi:10.1641/0006-
406 3568(2006)56[987:agcse]2.0.co;2

407 4. Mcleod E, Chmura GL, Bouillon S, Salm R, Björk M, Duarte CM, et al. A blueprint for blue
408 carbon: toward an improved understanding of the role of vegetated coastal habitats in
409 sequestering CO₂. *Front Ecol Environ*. 2011;9: 552–560. doi:10.1890/110004

410 5. Trivedi P, Batista BD, Bazany KE, Singh BK. Plant–microbiome interactions under a
411 changing world: responses, consequences and perspectives. *New Phytol*. 2022;234: 1951–
412 1959. doi:10.1111/nph.18016

413 6. Vandenkoornhuyse P, Quaiser A, Duhamel M, Le Van A, Dufresne A. The importance of
414 the microbiome of the plant holobiont. *New Phytol*. 2015;206: 1196–1206.
415 doi:10.1111/nph.13312

416 7. Compant S, Samad A, Faist H, Sessitsch A. A review on the plant microbiome: Ecology,
417 functions, and emerging trends in microbial application. *J Advert Res*. 2019;19: 29–37.
418 doi:10.1016/j.jare.2019.03.004

419 8. Fahimipour AK, Kardish MR, Lang JM, Green JL, Eisen JA, Stachowicz JJ. Global-Scale
420 Structure of the Eelgrass Microbiome. *Appl Environ Microbiol*. 2017;83.
421 doi:10.1128/AEM.03391-16

422 9. Ettinger CL, Voerman SE, Lang JM, Stachowicz JJ, Eisen JA. Microbial communities in
423 sediment from *Zostera marina* patches, but not the leaf or root microbiomes, vary in relation
424 to distance from patch edge. *PeerJ*. 2017;5: e3246. doi:10.7717/peerj.3246

425 10. Cúcio C, Engelen AH, Costa R, Muyzer G. Rhizosphere Microbiomes of European
426 Seagrasses Are Selected by the Plant, But Are Not Species Specific. *Front Microbiol*.
427 2016;7: 440. doi:10.3389/fmicb.2016.00440

428 11. Cúcio C, Overmars L, Engelen AH, Muyzer G. Metagenomic Analysis Shows the Presence
429 of Bacteria Related to Free-Living Forms of Sulfur-Oxidizing Chemolithoautotrophic
430 Symbionts in the Rhizosphere of the Seagrass *Zostera marina*. *Front Mar Sci*. 2018;5:
431 343793. doi:10.3389/fmars.2018.00171

432 12. Crump BC, Wojahn JM, Tomas F, Mueller RS. Metatranscriptomics and Amplicon
433 Sequencing Reveal Mutualisms in Seagrass Microbiomes. *Front Microbiol*. 2018;9: 332425.
434 doi:10.3389/fmicb.2018.00388

435 13. Hurtado-McCormick V, Kahlke T, Petrou K, Jeffries T, Ralph PJ, Seymour JR. Regional
436 and Microenvironmental Scale Characterization of the Seagrass Microbiome. *Front*

437 Microbiol. 2019;10: 1011. doi:10.3389/fmicb.2019.01011

438 14. Ettinger CL, Williams SL, Abbott JM, Stachowicz JJ, Eisen JA. Microbiome succession
439 during ammonification in eelgrass bed sediments. PeerJ. 2017;5: e3674.
440 doi:10.7717/peerj.3674

441 15. Sun F, Zhang X, Zhang Q, Liu F, Zhang J, Gong J. Seagrass (*Zostera marina*) Colonization
442 Promotes the Accumulation of Diazotrophic Bacteria and Alters the Relative Abundances of
443 Specific Bacterial Lineages Involved in Benthic Carbon and Sulfur Cycling. Appl Environ
444 Microbiol. 2015;81. doi:10.1128/AEM.01382-15

445 16. Wang L, Tomas F, Mueller RS. Nutrient enrichment increases size of *Zostera marina*
446 shoots and enriches for sulfur and nitrogen cycling bacteria in root-associated microbiomes.
447 FEMS Microbiol Ecol. 2020;96. doi:10.1093/femsec/fiaa129

448 17. Mohr W, Lehnen N, Ahmerkamp S, Marchant HK, Graf JS, Tschitschko B, et al. Terrestrial-
449 type nitrogen-fixing symbiosis between seagrass and a marine bacterium. Nature.
450 2021;600: 105–109. doi:10.1038/s41586-021-04063-4

451 18. Kristensen DM, Mushegian AR, Dolja VV, Koonin EV. New dimensions of the virus world
452 discovered through metagenomics. Trends Microbiol. 2010;18.
453 doi:10.1016/j.tim.2009.11.003

454 19. Jin M, Guo X, Zhang R, Qu W, Gao B, Zeng R. Diversities and potential biogeochemical
455 impacts of mangrove soil viruses. Microbiome. 2019;7. doi:10.1186/s40168-019-0675-9

456 20. Hurwitz BL, Westveld AH, Brum JR, Sullivan MB. Modeling ecological drivers in marine
457 viral communities using comparative metagenomics and network analyses. Proc Natl Acad
458 Sci U S A. 2014;111. doi:10.1073/pnas.1319778111

459 21. Breitbart MYA, Thompson LR, Suttle CA, Sullivan MB. Exploring the vast diversity of
460 marine viruses. Oceanography. 2007;20: 135–139. Available:
461 <https://www.jstor.org/stable/24860053>

462 22. Ettinger CL, Eisen JA. Characterization of the Mycobiome of the Seagrass, *Zostera marina*,
463 Reveals Putative Associations With Marine Chytrids. Front Microbiol. 2019;10: 2476.
464 doi:10.3389/fmicb.2019.02476

465 23. Bushnell B. BBTools. 2022. Available: <https://sourceforge.net/projects/bbmap/>

466 24. Ma X, Olsen JL, Reusch TBH, Procaccini G, Kudrna D, Williams M, et al. Improved
467 chromosome-level genome assembly and annotation of the seagrass, *Zostera marina*
468 (eelgrass). F1000Res. 2021;10. doi:10.12688/f1000research.38156.1

469 25. Langmead B, Trapnell C, Pop M, Salzberg SL. Ultrafast and memory-efficient alignment of
470 short DNA sequences to the human genome. Genome Biology. 2009;10: R25.
471 doi:10.1186/gb-2009-10-3-r25

472 26. Li H, Handsaker B, Wysoker A, Fennell T, Ruan J, Homer N, et al. The Sequence
473 Alignment/Map format and SAMtools. Bioinformatics. 2009;25: 2078–2079.
474 doi:10.1093/bioinformatics/btp352

475 27. Li D, Liu C-M, Luo R, Sadakane K, Lam T-W. MEGAHIT: an ultra-fast single-node solution

476 for large and complex metagenomics assembly via succinct de Bruijn graph. *Bioinformatics*.
477 2015;31: 1674–1676. doi:10.1093/bioinformatics/btv033

478 28. Eren AM, Murat Eren A, Esen ÖC, Quince C, Vineis JH, Morrison HG, et al. Anvi'o: an
479 advanced analysis and visualization platform for 'omics data. *PeerJ*. 2015;3: e1319.
480 doi:10.7717/peerj.1319

481 29. Hyatt D, Chen G-L, Locascio PF, Land ML, Larimer FW, Hauser LJ. Prodigal: prokaryotic
482 gene recognition and translation initiation site identification. *BMC Bioinformatics*. 2010;11:
483 119. doi:10.1186/1471-2105-11-119

484 30. Lee MD. GToTree: a user-friendly workflow for phylogenomics. *Bioinformatics*. 2019;35:
485 4162–4164. doi:10.1093/bioinformatics/btz188

486 31. Lee MD. GToTree: a user-friendly workflow for phylogenomics. *Bioinformatics*. 2019;35:
487 4162–4164. doi:10.1093/bioinformatics/btz188

488 32. Delmont T. Assessing the completion of eukaryotic bins with anvi'o. 2018. Available:
489 <http://merenlab.org/delmont-euk-scgs>

490 33. Eddy SR. Accelerated Profile HMM Searches. *PLoS Comput Biol*. 2011;7: e1002195.
491 doi:10.1371/journal.pcbi.1002195

492 34. Seemann T. barrnap: BAsic Rapid Ribosomal RNA Predictor. Available:
493 <https://github.com/tseemann/barrnap>

494 35. Menzel P, Ng KL, Krogh A. Fast and sensitive taxonomic classification for metagenomics
495 with Kaiju. *Nat Commun*. 2016;7: 11257. doi:10.1038/ncomms11257

496 36. Alneberg J, Bjarnason BS, de Bruijn I, Schirmer M, Quick J, Ijaz UZ, et al. Binning
497 metagenomic contigs by coverage and composition. *Nat Methods*. 2014;11: 1144–1146.
498 doi:10.1038/nmeth.3103

499 37. Kang DD, Li F, Kirton E, Thomas A, Egan R, An H, et al. MetaBAT 2: an adaptive binning
500 algorithm for robust and efficient genome reconstruction from metagenome assemblies.
501 *PeerJ*. 2019;7: e7359. doi:10.7717/peerj.7359

502 38. Graham ED, Heidelberg JF, Tully BJ. BinSanity: unsupervised clustering of environmental
503 microbial assemblies using coverage and affinity propagation. *PeerJ*. 2017;5: e3035.
504 doi:10.7717/peerj.3035

505 39. Wu Y-W, Tang Y-H, Tringe SG, Simmons BA, Singer SW. MaxBin: an automated binning
506 method to recover individual genomes from metagenomes using an expectation-
507 maximization algorithm. *Microbiome*. 2014;2: 1–18. doi:10.1186/2049-2618-2-26

508 40. Sieber CMK, Probst AJ, Sharrar A, Thomas BC, Hess M, Tringe SG, et al. Recovery of
509 genomes from metagenomes via a dereplication, aggregation, and scoring strategy. *Nature
510 Microbiology*. 2018;3: 836–843. doi:10.1101/107789

511 41. Nayfach S, Shi ZJ, Seshadri R, Pollard KS, Kyrpides NC. New insights from uncultivated
512 genomes of the global human gut microbiome. *Nature*. 2019;568: 505–510.
513 doi:10.1038/s41586-019-1058-x

514 42. Parks DH, Imelfort M, Skennerton CT, Hugenholtz P, Tyson GW. CheckM: assessing the
515 quality of microbial genomes recovered from isolates, single cells, and metagenomes.
516 *Genome Res.* 2015;25: 1043–1055. doi:10.1101/gr.186072.114

517 43. Chklovski A, Parks DH, Woodcroft BJ, Tyson GW. CheckM2: a rapid, scalable and
518 accurate tool for assessing microbial genome quality using machine learning. *Nat Methods.*
519 2023;20: 1203–1212. doi:10.1038/s41592-023-01940-w

520 44. Bowers RM, Kyrpides NC, Stepanauskas R, Harmon-Smith M, Doud D, Reddy TBK, et al.
521 Minimum information about a single amplified genome (MISAG) and a metagenome-
522 assembled genome (MIMAG) of bacteria and archaea. *Nat Biotechnol.* 2017;35: 725–731.
523 doi:10.1038/nbt.3893

524 45. Chaumeil P-A, Mussig AJ, Hugenholtz P, Parks DH. GTDB-Tk: a toolkit to classify
525 genomes with the Genome Taxonomy Database. *Bioinformatics.* 2019.
526 doi:10.1093/bioinformatics/btz848

527 46. Sogin EM, Michelod D, Gruber-Vodicka HR, Bourceau P, Geier B, Meier DV, et al. Sugars
528 dominate the seagrass rhizosphere. *Nature Ecology & Evolution.* 2022;6: 866–877.
529 doi:10.1038/s41559-022-01740-z

530 47. Rubio-Portillo E, Martin-Cuadrado A-B, Ramos-Esplá AÁ, Antón J. Metagenomics Unveils
531 *Posidonia oceanica* “Banquettes” as a Potential Source of Novel Bioactive Compounds and
532 Carbohydrate Active Enzymes (CAZymes). *mSystems.* 2021.
533 doi:10.1128/msystems.00866-21

534 48. Miranda K, Weigel BL, Fogarty EC, Veseli IA, Giblin AE, Murat Eren A, et al. The Diversity
535 and Functional Capacity of Microbes Associated with Coastal Macrophytes. *mSystems.*
536 2022. doi:10.1128/msystems.00592-22

537 49. Schorn S, Ahmerkamp S, Bullock E, Weber M, Lott C, Liebeke M, et al. Diverse
538 methylotrophic methanogenic archaea cause high methane emissions from seagrass
539 meadows. *Proceedings of the National Academy of Sciences.* 2022;119: e2106628119.
540 doi:10.1073/pnas.2106628119

541 50. Fraser MW, Martin BC, Wong HL, Burns BP, Kendrick GA. Sulfide intrusion in a habitat
542 forming seagrass can be predicted from relative abundance of sulfur cycling genes in
543 sediments. *Sci Total Environ.* 2023;864: 161144. doi:10.1016/j.scitotenv.2022.161144

544 51. Fraser MW, Gleeson DB, Grierson PF, Laverock B, Kendrick GA. Metagenomic Evidence
545 of Microbial Community Responsiveness to Phosphorus and Salinity Gradients in Seagrass
546 Sediments. *Front Microbiol.* 2018;9: 378381. doi:10.3389/fmicb.2018.01703

547 52. Guo J, Vik D, Pratama AA, Roux S, Sullivan M. Viral sequence identification SOP with
548 VirSorter2. *protocols.io.* 2021. Available: <https://www.protocols.io/view/viral-sequence-identification-sop-with-virsorter2-btv8nn9w>

549 53. Guo J, Bolduc B, Zayed AA, Varsani A, Dominguez-Huerta G, Delmont TO, et al.
550 VirSorter2: a multi-classifier, expert-guided approach to detect diverse DNA and RNA
551 viruses. *Microbiome.* 2021;9: 37. doi:10.1186/s40168-020-00990-y

552 54. Nayfach S, Camargo AP, Schulz F, Eloë-Fadrosh E, Roux S, Kyrpides NC. CheckV

554 assesses the quality and completeness of metagenome-assembled viral genomes. *Nat*
555 *Biotechnol.* 2021;39: 578–585. doi:10.1038/s41587-020-00774-7

556 55. Shaffer M, Borton MA, McGivern BB, Zayed AA, La Rosa SL, Soden LM, et al. DRAM for
557 distilling microbial metabolism to automate the curation of microbiome function. *Nucleic*
558 *Acids Res.* 2020;48: 8883–8900. doi:10.1093/nar/gkaa621

559 56. Olm MR, Brown CT, Brooks B, Banfield JF. dRep: a tool for fast and accurate genomic
560 comparisons that enables improved genome recovery from metagenomes through de-
561 replication. *ISME J.* 2017;11: 2864–2868. doi:10.1038/ismej.2017.126

562 57. Bin Jang H, Bolduc B, Zablocki O, Kuhn JH, Roux S, Adriaenssens EM, et al. Taxonomic
563 assignment of uncultivated prokaryotic virus genomes is enabled by gene-sharing
564 networks. *Nat Biotechnol.* 2019;37: 632–639. doi:10.1038/s41587-019-0100-8

565 58. Cook R, Brown N, Redgwell T, Rihtman B, Barnes M, Clokie M, et al. INfrastructure for a
566 PHAge REference Database: Identification of Large-Scale Biases in the Current Collection
567 of Cultured Phage Genomes. *PHAGE.* 2021;2: 214–223. doi:10.1089/phage.2021.0007

568 59. Camargo AP, Roux S, Schulz F, Babinski M, Xu Y, Hu B, et al. Identification of mobile
569 genetic elements with geNomad. *Nat Biotechnol.* 2024;42: 1303–1312.
570 doi:10.1038/s41587-023-01953-y

571 60. Roux S, Camargo AP, Coutinho FH, Dabdoub SM, Dutilh BE, Nayfach S, et al. iPHoP: An
572 integrated machine learning framework to maximize host prediction for metagenome-
573 derived viruses of archaea and bacteria. *PLoS Biol.* 2023;21: e3002083.
574 doi:10.1371/journal.pbio.3002083

575 61. Langmead B, Salzberg SL. Fast gapped-read alignment with Bowtie 2. *Nature methods.*
576 2012;9. doi:10.1038/nmeth.1923

577 62. Quinlan AR, Hall IM. BEDTools: a flexible suite of utilities for comparing genomic features.
578 *Bioinformatics.* 2010;26: 841–842. doi:10.1093/bioinformatics/btq033

579 63. Roux S, Adriaenssens EM, Dutilh BE, Koonin EV, Kropinski AM, Krupovic M, et al.
580 Minimum Information about an Uncultivated Virus Genome (MIUViG). *Nat Biotechnol.*
581 2018;37: 29–37. doi:10.1038/nbt.4306

582 64. Roux S, Emerson JB, Eloë-Fadrosch EA, Sullivan MB. Benchmarking viromics: an
583 evaluation of metagenome-enabled estimates of viral community composition and diversity.
584 *PeerJ.* 2017;5: e3817. doi:10.7717/peerj.3817

585 65. R Core Team. R: A Language and Environment for Statistical Computing. 2021. Available:
586 <https://www.r-project.org/>

587 66. McMurdie PJ, Holmes S. phyloseq: An R Package for Reproducible Interactive Analysis
588 and Graphics of Microbiome Census Data. *PLoS One.* 2013;8: e61217.
589 doi:10.1371/journal.pone.0061217

590 67. Wickham H, Averick M, Bryan J, Chang W, McGowan LD, François R, et al. Welcome to
591 the Tidyverse. *Journal of Open Source Software.* 2019;4: 1686. doi:10.21105/joss.01686

592 68. Lahti L, Shetty S. Tools for microbiome analysis in R - Microbiome package. 2017.

593 Available: <http://microbiome.github.com/microbiome>

594 69. Turner D, Kropinski AM, Adriaenssens EM. A Roadmap for Genome-Based Phage
595 Taxonomy. *Viruses*. 2021;13. doi:10.3390/v13030506

596 70. Santos-Medellin C, Zinke LA, Ter Horst AM, Gelardi DL, Parikh SJ, Emerson JB. Viromes
597 outperform total metagenomes in revealing the spatiotemporal patterns of agricultural soil
598 viral communities. *ISME J*. 2021;15: 1956–1970. doi:10.1038/s41396-021-00897-y

599 71. Ettinger CL, Saunders M, Selbmann L, Delgado-Baquerizo M, Donati C, Albanese D, et al.
600 Highly diverse and unknown viruses may enhance Antarctic endoliths' adaptability.
601 *Microbiome*. 2023;11: 103. doi:10.1186/s40168-023-01554-6

602 72. An L, Liu X, Wang J, Xu J, Chen X, Liu X, et al. Global diversity and ecological functions of
603 viruses inhabiting oil reservoirs. *Nat Commun*. 2024;15: 6789. doi:10.1038/s41467-024-
604 51101-6

605

606

607

608

609

610

611

612

613

614

615

616

617

618

619

620

621

622

623

624

625

626

627

628

629

630

631

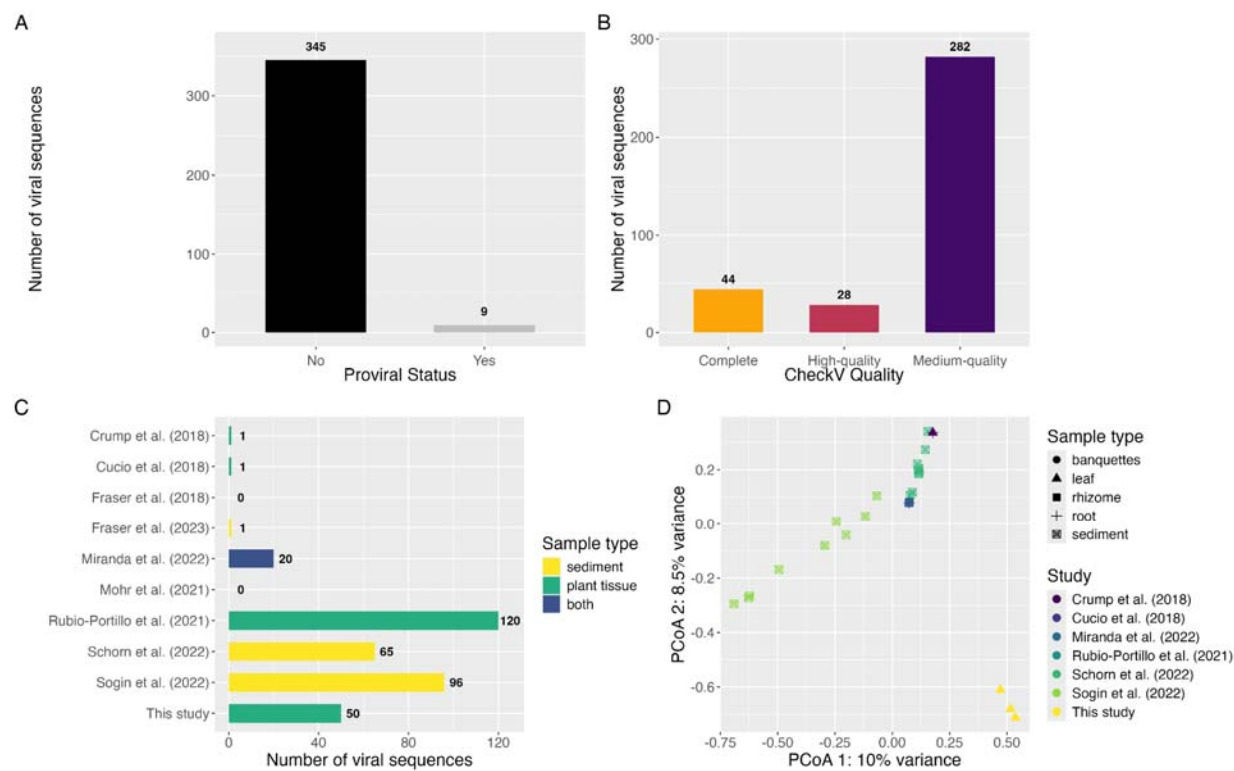
632

633

634

635 **Figure 1.** Putative viral sequences identified from seagrass ecosystems. (A) The proviral status
636 of predicted viral genomes is shown as a bar graph, with the number above the bar representing
637 the total number of sequences. (B) CheckV quality metrics for viral sequences are shown as a
638 bar graph with bars colored by quality and the number above the bar representing the total
639 number of sequences in each bar. (C) Bar chart depicting the number of viral sequences
640 identified in the metagenomic co-assembly from each study, with the number to the right of the
641 bar representing the total number of sequences in each bar. (D) Principal-coordinate analysis
642 (PCoA) visualization of Hellinger distances of relative abundance of viral communities across
643 metagenomic samples. Samples are colored by study, and have shapes based on sample type.

644



645

646

647

648

649

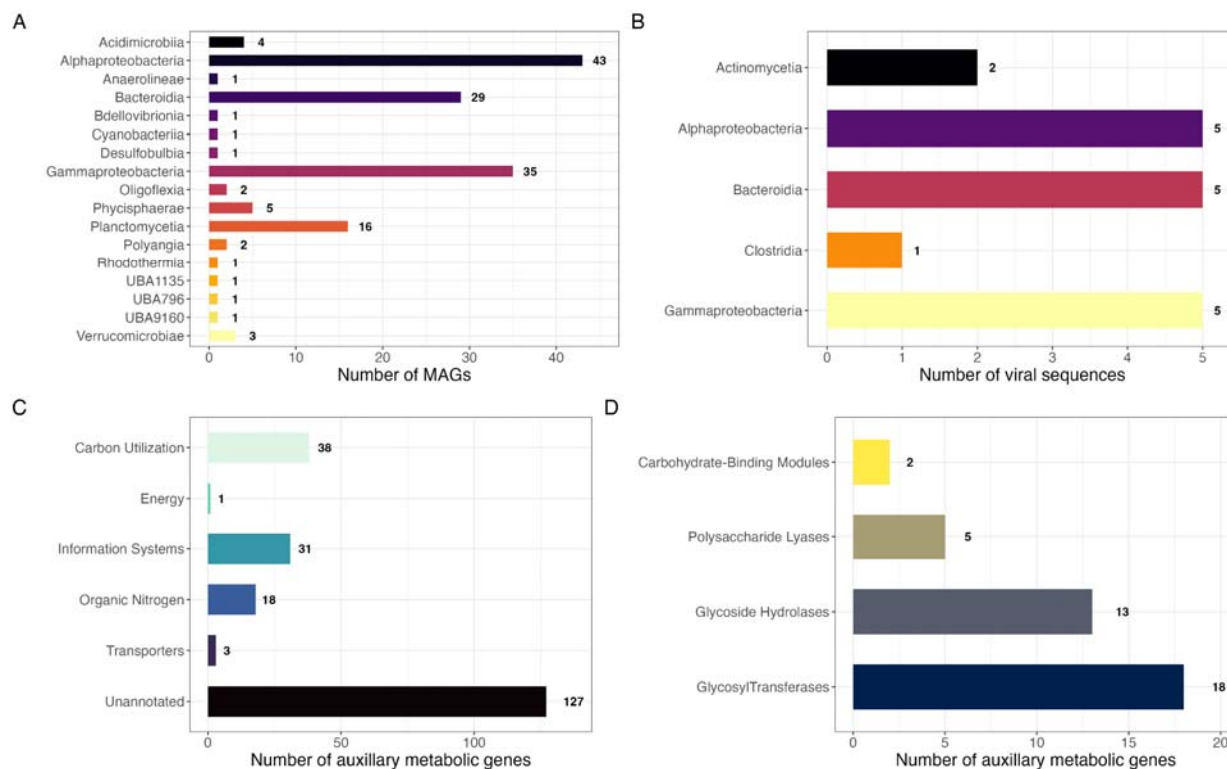
650

651

652

653 **Figure 2.** Viral-Bacterial interactions likely related to carbon metabolism. (A) Bar chart depicting
654 the number of metagenome-assembled genomes (MAGs) identified in this study, colored by
655 taxonomic class, and with the number to the right of the bar representing the total number of
656 MAGs in each bar. (B) Bar chart depicting the viral host predictions, colored by host taxonomic
657 class, and with the number to the right of the bar representing the total number of viral
658 sequences in each bar. (C) Bar chart showing the number of predicted phage auxiliary
659 metabolic genes (AMGs) summarized by DRAM-v distilled metabolic categories, with the
660 number to the right of the bar representing the total number of AMGs in each bar. (D) Bar chart
661 showing the number of predicted phage AMGs in different CAZyme families with-in the carbon
662 utilization category, with the number to the right of the bar representing the total number of
663 AMGs in each bar.

664



665

666

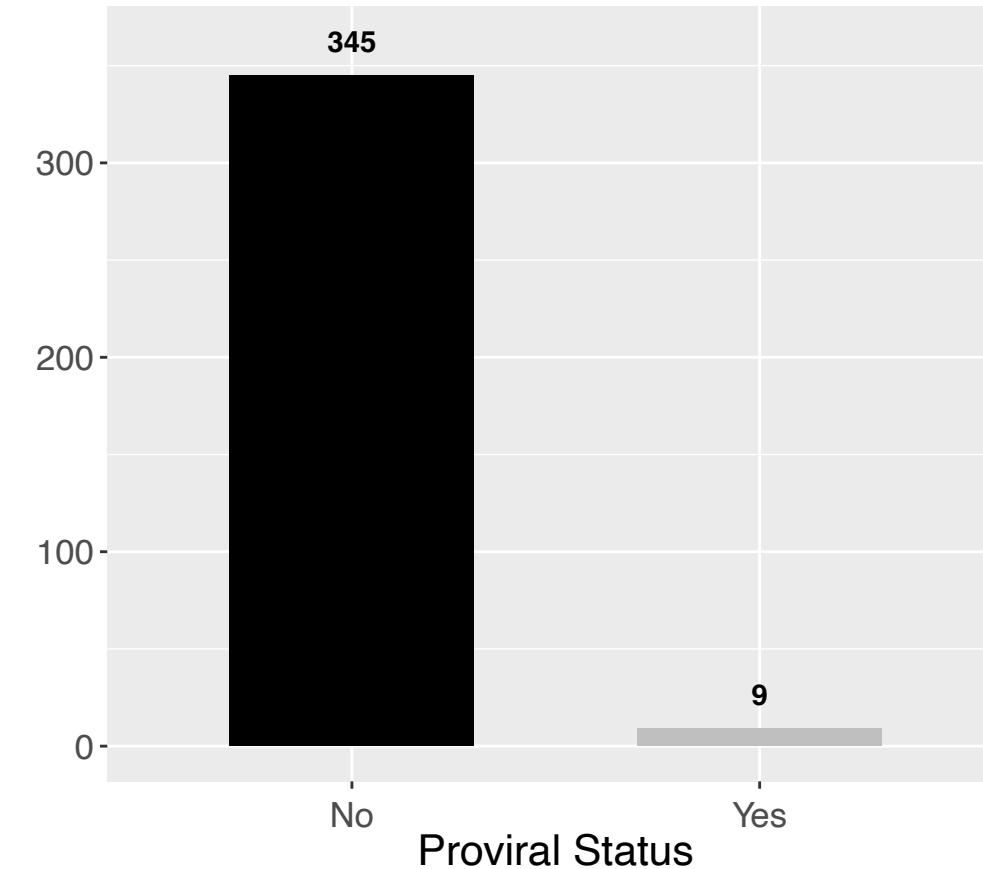
667

668

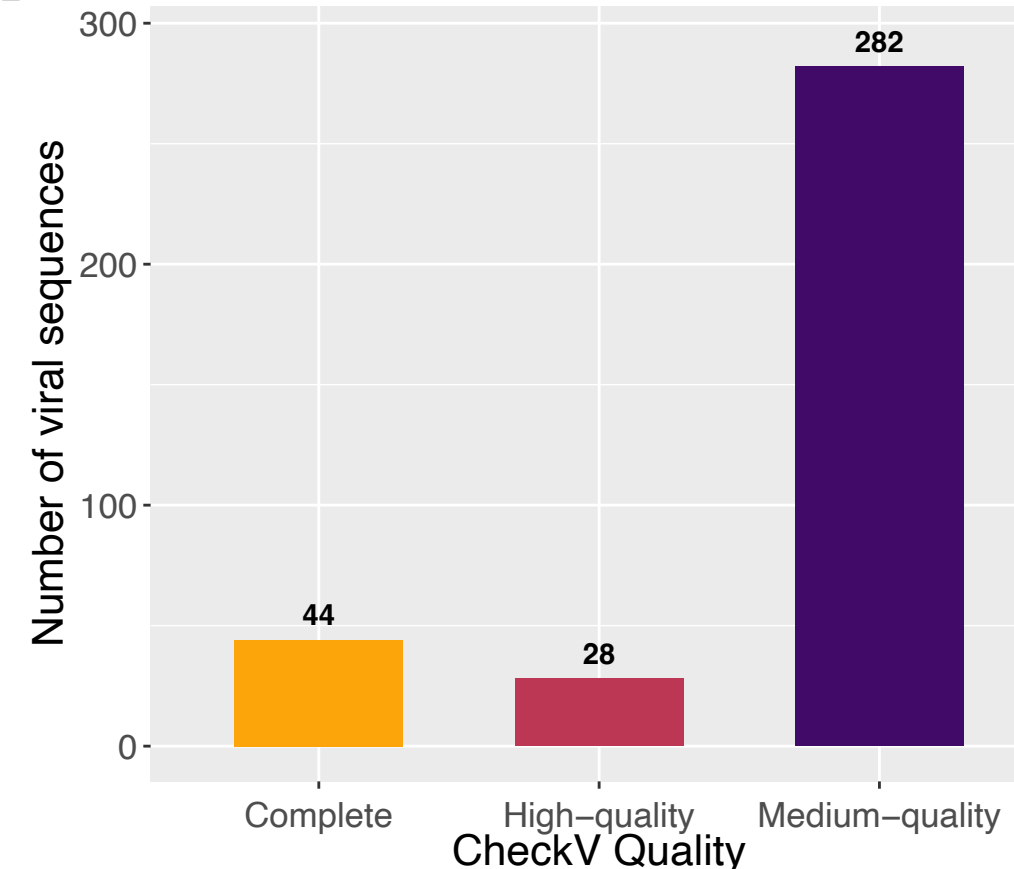
669

A

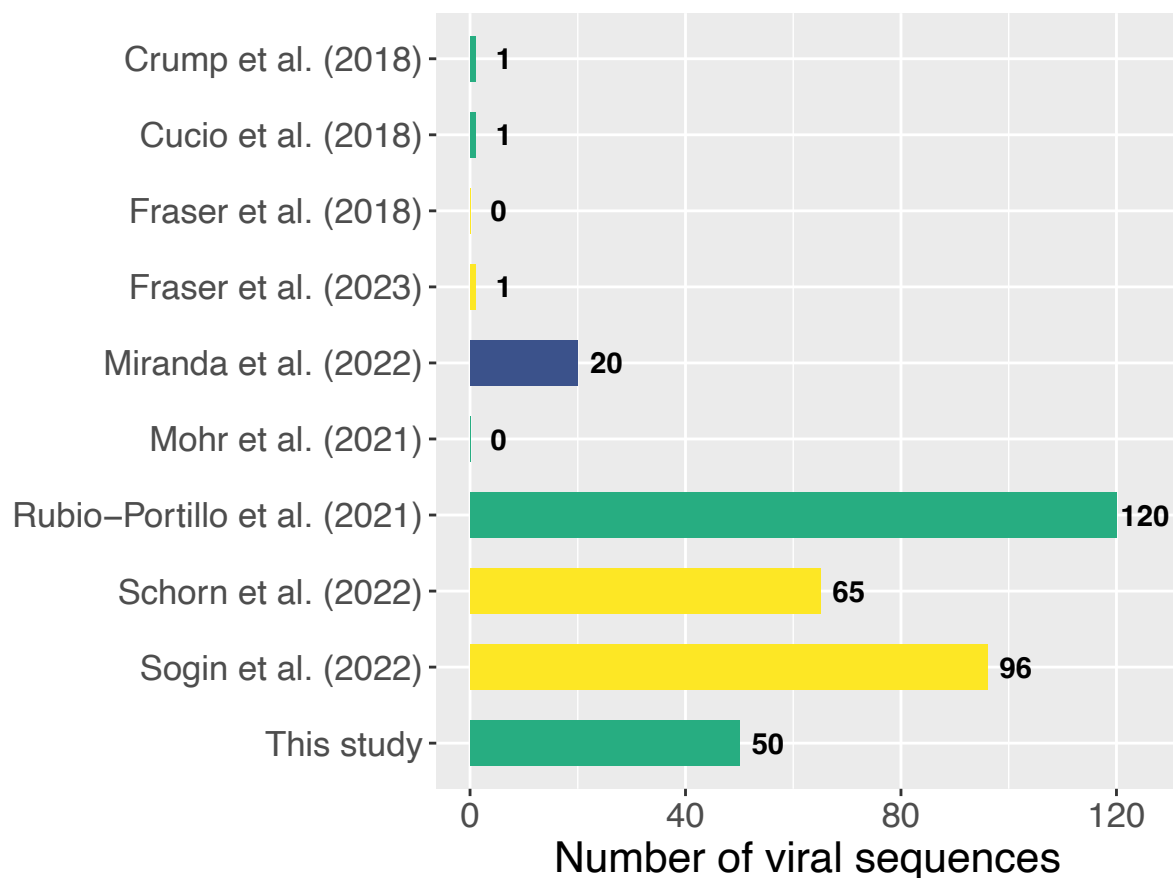
Number of viral sequences



B

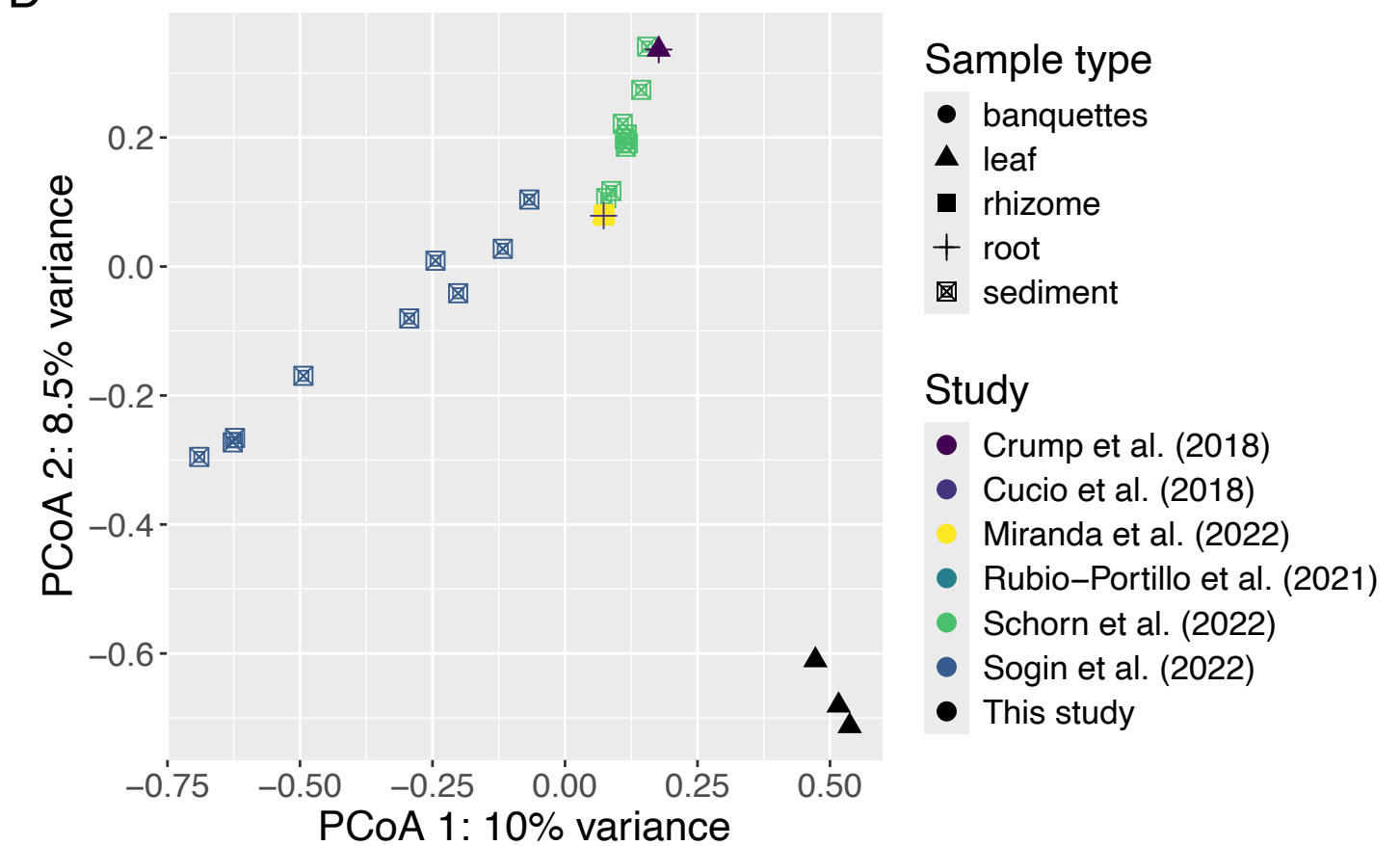


C

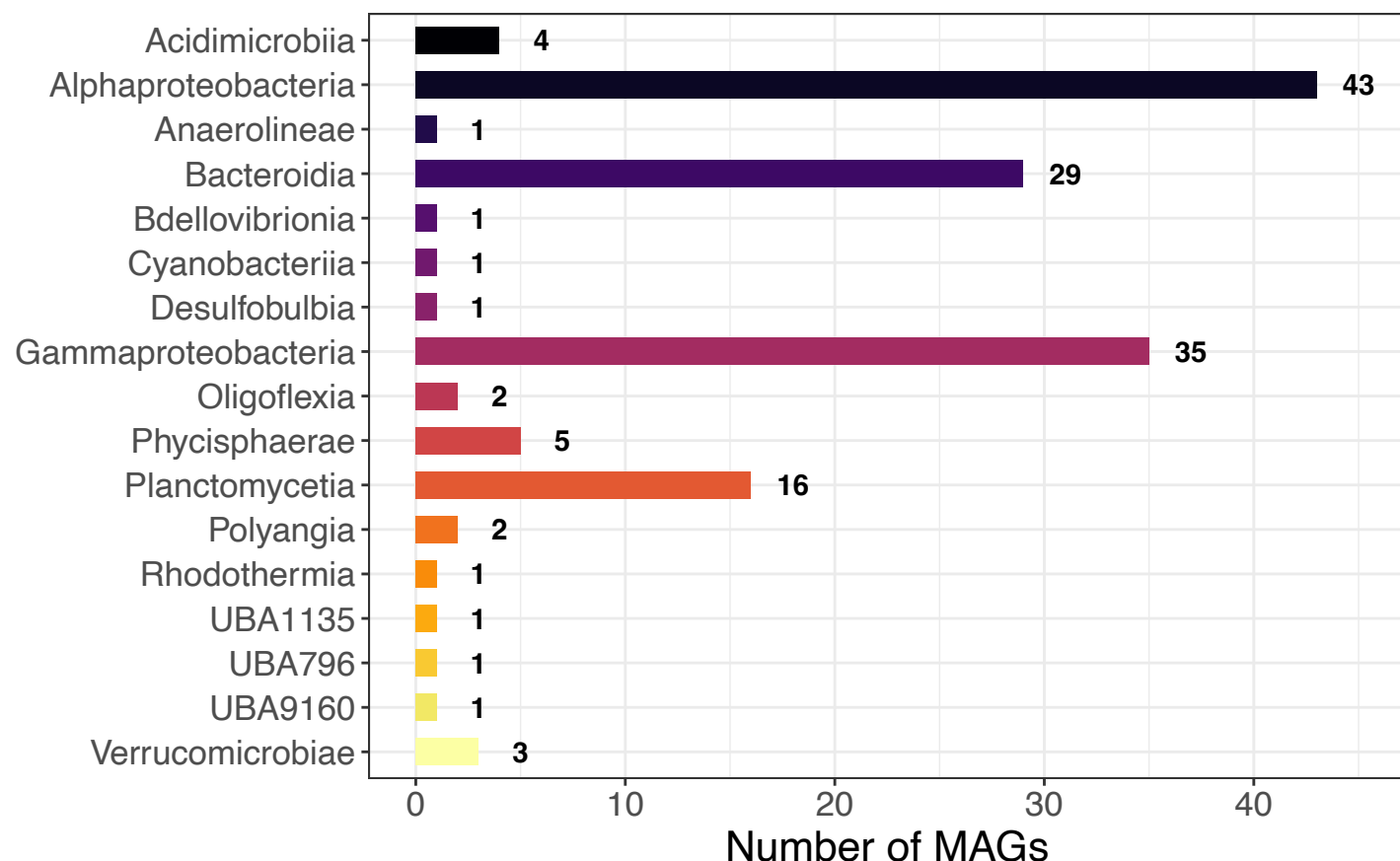


Sample type
 sediment
 plant tissue
 both

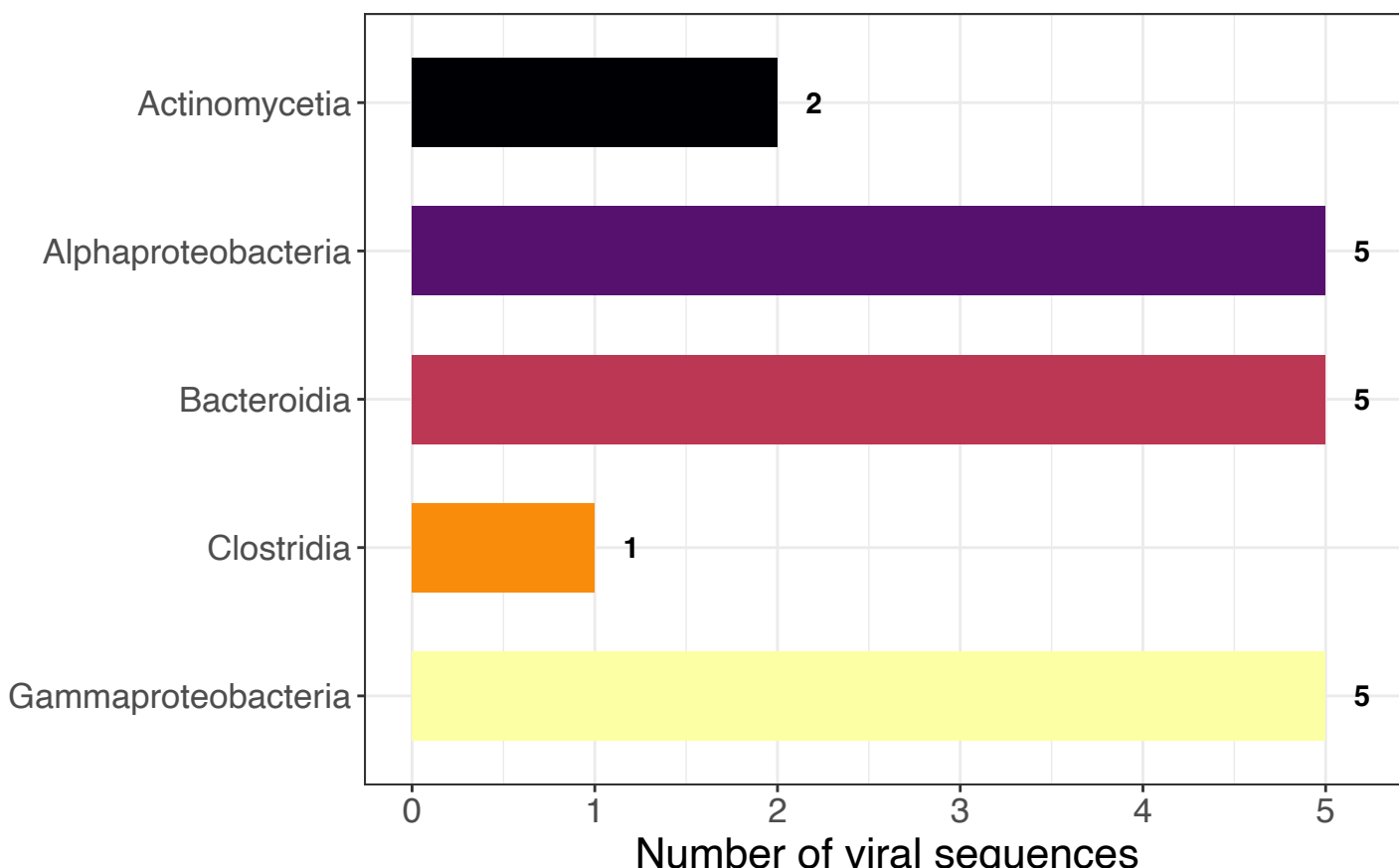
D



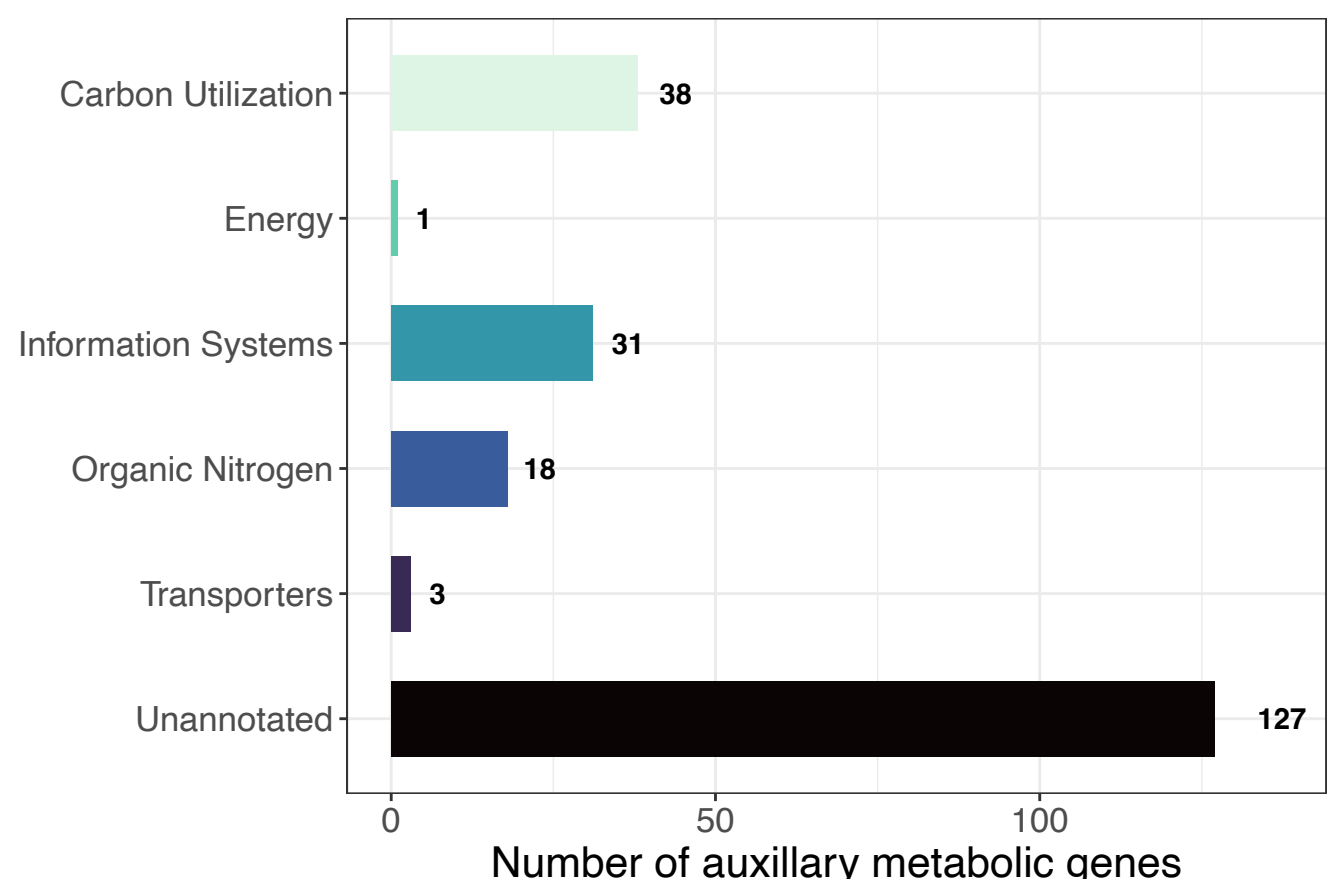
A



B



C



D

